

Development of 3-Dimensional MC Ion Implantation Simulator

Myung-Sik Son and Ho-Jung Hwang

Semiconductor Process and Device Laboratory
Dept. of Electronics Engineering, Chung-Ang University

Introduction

The continued scaling of feature size in the ULSI device technology has required shallower, more compact impurity profiles, and more precisely controlled doping profiles. In addition, the implant-induced damage has large effect on the impurity diffusion such as TED (Transient Enhanced Diffusion) phenomena during thermal annealing after ion implantation. As a result, greatly reduced thermal budgets are necessary for the development and manufacturing of ULSI devices. For this reason, an accurate and efficient physically-based 3D model capable of predicting the as-implanted dopant and the defect profiles under the implanted area becomes highly desirable.

In this paper are presented a newly proposed 3D Monte Carlo(MC) damage model for the dynamic simulation based on the implant-induced point defect distributions in crystalline silicon. This model was applied to low energy B, BF₂, P, and As implants for the formation of the shallow junction for the ULSI CMOS technology development. In addition, a newly applied 3D trajectory split method was implemented into our model to reduce the statistical fluctuations of the implanted impurity and the defect profiles in the relatively large implanted area as compared to 1D or 2D simulations. The 3D formation of the amorphous region and the ultra-shallow junction around the implanted region could be predicted by using our model, TRICSI(Transport Ions into Crystal-Silicon). The model has two improvements for the 3D dynamic simulation. It has no limitation of the simulation dimensions and used less computer memory. Typically, the required memory in our code is about 32Mbyte.

3D Model Development

To more accurately predict the cumulative damage, and more dynamically simulate the channelling, dechannelling and rechanneling process of the moving atoms during ion implantation, all of the trajectories of both the implanted ions and the recoiled silicons are directly followed. As considered the recombination between the vacancy and the interstitial, each information of the produced vacancies and interstitials during the binary collision process is saved in each unit volume($\Delta x \Delta y \Delta z$) for both the vacancy and the interstitial. With this statistical information of the point defects, the damaged silicon lattices are modeled by introducing the surviving vacancy probability $P_v(x,y,z)$ and the safely existing interstitial probability $P_i(x,y,z)$ in the local volume to affect the movings of the implanted ions and the recoiled silicons.

Instead of choosing the tetrahedral sites for interstitial site, the model creates the random interstitial sites defined as the sites except for the ideal silicon sites. The length of FPLS(the flight-path length in the ideal crystal structure) is first searched in the ideal crystal silicon in

the local volume, and then the interstitials are created like the following formula (1) if the random number R_n is content with the condition of the equation of $R_n < P_i(x,y,z) : L_s = (FPLS - R_{cap})R_n + R_{cap}$ (1), where L_s is the length from the position of the previous collision atom. The R_{cap} is the capture radius for the vacancy-interstitial recombination[1]. After failing in searching the interstitial described above, it is checked for the vacancy generation whether the collision silicon position in the ideal crystal structure is occupied by a vacancy. The following condition is used: $R_n < P_v(x,y,z)$ (2). The above described sequence for each collision step with the interstitial or the stationary silicon or the vacancy is repeated until the local region is completely amorphized. After the region is amorphized, the amorphous model[2] is used. The amorphous criteria in the local volume is defined as the point defect concentration of $N_v + N_i$ is reached to and over the saturation concentration N_{sat} of the point defect, which is determined by the R_{cap} [1]. We used 0.54 times silicon lattice constant for all dopant implants. The self-annealing of the defect recombination during ion implantation at room temperature is considered, which resulted in the saturation concentration N_{sat} for the point defect[1]. We defined the interstitial recombination probability $P_{RINT}(x,y,z)$ ($= N_{vac} / N_{sat}$) at the interstitial generation, and the vacancy recombination probability $P_{RVAC}(x,y,z)$ ($= N_{int} / N_{sat}$) at the interstitial generation, where N_{vac} and N_{int} is the safely existed interstitial and the previously created vacancy probability in the local volume, respectively. The following conditions of equations (3), (4) are used for checking the defect recombination at each defect generation: For each vacancy generation, the recombination condition with the previously existed interstitials is checked by generating the random number in the following equation: $R_n < P_{RINT}(x,y,z)$ (3). For each interstitial generation, the recombination condition with the previously existed vacancies is checked by generating the random number in the following equation: $R_n < P_{RVAC}(x,y,z)$ (4).

In order to reduce the statistical fluctuations in the 3D distributions of both the impurity and the defect due to the lack of the simulated particles in the large area, the trajectory split method are three-dimensionally applied in our dynamic damage model. Our simple approach for the trajectory split method is similar to that of the UT-MARLOWE[3], but the different virtual split criteria are used and the split levels based on the range profile are extended to two lateral directions. In our technique, several equi-depths(D_1, D_2, \dots, D_n) to the X depth direction and the lateral equi-distances(L_1, L_2, \dots, L_n) to the Z- and the Y- lateral directions from the deviated region from each mask edge, not the implanted square region, are chosen. The n is 10 used. The lateral equi-distance is the same to two lateral directions and used by half of the distance of a equi-depth level. Because of these lateral splits, the lateral fluctuations from the mask edges are more successfully reduced as showed in Fig. 3.

The full-dynamic simulation on each virtual split branches is made by the above described full-dynamic

damage model and also, all of the recoiled silicons made by the split branches are explicitly followed. Therefore, the fluctuation of the defect distribution is more reduced as showed in Fig. 3. Our model explicitly takes into account the generation and recombination of point defects, the amorphization of the crystal, and the channel blocking by the implant-induced damage. The new full-dynamic damage model predicts well the impurity range profile dependence on the dose in the different dopant implants as showed in Fig. 1(a). for Boron, Fig. 1(b). for BF_2 , and Fig. 2. for Arsenic, as the results obtaining by the 3D simulations are compared to the 1D SIMS experiments[3-5].

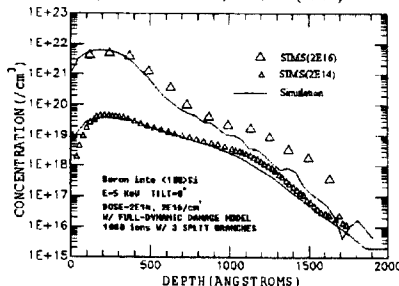
Results and Conclusions

In our results, the point defect distributions are less than those of the modified Kinchin-Pease approach[2], and the vacancy distributions differ from the interstitial distributions for all simulation cases at the different dopant implants[6]. In details, the vacancy and the interstitial distributions differs from each other to and from the peak damage range. As an example for the above description of the damage distribution. we showed the As-implanted impurity and the As-produced damage profiles at tilt 10° implants as showed Fig. 2. The results show that the vacancy concentrations are higher than the interstitial ones from the surface to the damage peak range just before the ion peak range, and, reversely, the interstitial concentrations are higher than the vacancy ones from the damage peak into the silicon bulk. We believe that this is due to the momentum of the implanted impurity, and so the recoiled silicons are directed more into the bulk, while the vacancies are left behind. In addition, the 0° tilt implant produces more defect than the 10° tilt case. This is the same result with the ref. [1].

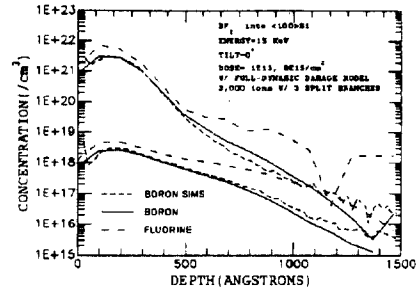
As a conclusion, the 3D formations of the amorphous region and the ultra-shallow junction for the ULSI device technology could be predicted by using our model, TRICSI(Transport Ions into Crystalline Silicon).

References

- [1] K.M. Klein, C.Park, A.F. Tasch, Nucl. Inst. and Meth., B59/60, 60 (1991)
- [2] J. F. Ziegler, J.P. Biersack, The stopping and Range of Ions in Solids, Vol. I, New York : Pergamon (1985)
- [3] S.-H. Yang et al, in Process Physics and Modeling in Semiconductor Technology/1996. G.R. Srinivasan, C.S. Murthy, and S.T. Dunham, Editors, PV96-4, p.481, The Electrochemical Society Proceedings Series, Pennington, NJ(1996)
- [4] M. Hane et al, IEEE IEDM91 Tech. Dig., 701(1991)
- [5] S.H. Yang et al. Nucl. Inst. and Meth., B102, 242(1995)
- [6] M. Servidori et al, Nucl. Inst. Meth., B22, 497(1987)



(a) B implant at energy 5 KeV, dose $2E14, 2E16/\text{cm}^2$, tilt 0° , rotation 0° .



(b) BF_2 implants at energy 15 KeV, dose $1E15, 8E15/\text{cm}^2$, tilt 0° , rotation 0° .

Fig. 1. Simulation results of B- and BF_2 -implanted profiles at low-dose case and high-dose case with the SIMS experiments[3-4].

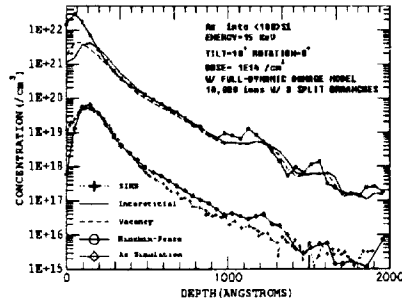


Fig. 2. Simulation results of the As-implanted range profiles and the As-implant-produced damage profiles at 10° tilt implant. The SIMS experiments are taken from Ref.[5].

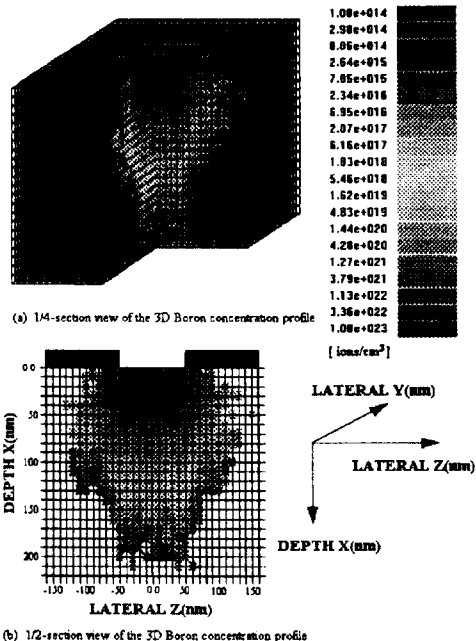


Fig. 3. 3D Boron concentration profiles at energy 5 KeV, dose $2E16/\text{cm}^2$, tilt 0° , rotation 0° , where the implanted square region which is $100 \times 100 \text{ nm}^2$.